Modulation of exciton states through resonant excitation by continuous wave lasers in a GaAs/AlAs multiple quantum well

Osamu Kojima[1], Takashi Kita[1], Matthew J. Steer[2] and Richard A. Hogg[2]

[1]Department of Electrical and Electronic Engineering, Graduate School of Engineering, Kobe University, 1-1 Rokkodai, Nada, Kobe 657-8501, Japan
[2]Electronics and Nanoscale Engineering, James Watt School of Engineering, University of Glasgow, Glasgow G12 8LT, United Kingdom

E-mail: kojima@phoenix.kobe-u.ac.jp

Abstract. Interactions between excitons with different energies are significant in device application, particularly in the emission of intense terahertz waves caused by difference frequency mixing. In this paper, the interactions of excitons generated by two resonant continuous-wave laser beams are assessed via the change in reflectivity. While calculations suggest that the reflectivity change depends on the exciton number, experimental results measured for various excitation powers, probe powers, and excitation energies (heavy-hole and light-hole excitons) show different profiles. Furthermore, the signals probed at a heavy-hole exciton differ from those at a light-hole exciton. These results indicate the importance of careful control of excitation levels for terahertz wave generation.

Submitted to: *J. Phys. D: Appl. Phys.*

1. Introduction

The temporal and spatial overlap of two excitons or polarizations is essential for nonlinear optics. When excitons are simply created with high density, scattering and collision processes trigger their annihilation. However, in the case of exciton overlap, interesting coherent oscillation phenomena occur. For excitons with different energies, such as heavy-hole (HH) and light-hole (LH) excitons, the overlap of simultaneously created excitons has been investigated based on quantum beats using ultrashort pulse lasers, as quantum beats are a typical temporal oscillation phenomena [1-18]. Moreover, Bloch oscillations also occur as coherent oscillations due to exciton overlap [19-22]. Here, for the quantum beat scheme, the overlap of simultaneously generated HH and LH excitons with frequencies of $\omega_{\rm HH}$ and $\omega_{\rm LH}$, respectively, is essential. Consequently, oscillation signals with a frequency of $|\omega_{\rm LH} - \omega_{\rm HH}|$ appear in pump-probe, four-wave-mixing, and terahertz (THz) wave signals.

Moreover, the overlap of two frequency polarizations can lead to THz wave emission due to difference-frequency mixing (DFM); the overlap of polarizations for frequencies ω_1 and ω_2 generates a wave with frequency $|\omega_1 - \omega_2|$ [23-27]. The DFM technique can effectively realize frequency-tunable THz wave systems [27-29]. For a DFM signal generated in a GaAs/AlAs multiple quantum well (MQW), the signal is enhanced close to the HH-exciton energy; when two lasers are tuned to the HH exciton within its inhomogeneous broadening width, the signal is enhanced, and the resonant effect of the simultaneous excitation of the HH and LH excitons is very weak. This trend suggests that the effect of the overlap of HH and LH excitons created by continuous-wave (cw) lasers is weaker than that of the quantum-beat-type overlap. Therefore, when the exciton overlap by cw excitation is clarified, THz signals can be enhanced. For instance, the interaction between two modes in a dual-frequency laser device has been investigated with respect to Lamb coupling [30-36]. which gives the information about interactions between excitons with different frequencies under cw excitation based on the reflectivity change. Thus, in this work, we explore the interactions between excitons excited by cw lasers at room temperature based on the reflectivity change signal. The reflectivity change varies with excitation power, probe power, and excitation energies (HH and LH excitons). By comparing our experimental findings with calculation results, we assess the interaction of excitons created by excitation and probe laser beams. Our results will aid in the enhancement of DFM signals using excitons.

2. Experiment

We used an undoped GaAs/AlAs MQW embedded in a p-i-n structure on a (001) n^+-doped GaAs substrate grown by molecular-beam epitaxy. The surface p-doped GaAs layer has a doping concentration of 1×10^{18} cm^{-3} and a thickness of 50 nm, while the bottom n-doped GaAs layer has a doping concentration of 3×10^{18} cm^{-3} and a thickness of 1500 nm. The MQW consists of 30 periods of GaAs and AlAs layers,

whose thickness is 7.25 nm. The details of the sample structure are available in our previous report [37]. To measure the reflectivity change, a cw-mode Ti:sapphire laser and semiconductor lasers were used as the excitation and probe light source, respectively, for normal incidence, corresponding the same setup used for DFW measurements. The experimental setup is schematically shown in Fig. 1. The energy of the Ti:sapphire laser was tuned from 1.490 to 1.540 eV, and its intensity was modulated by a light chopper at approximately 1 kHz. Semiconductor lasers with photon energies corresponding to the exciton energies were used as the probe light. To maintain the laser intensities constant, a laser power stabilizer for the Ti:sapphire laser was used and the semiconductor lasers have the cooling system. The two beams were combined on a half mirror in free space with the same polarization, and the combined beam was focused on the sample surface through a hole in an off-axis parabolic mirror. To eliminate Rayleigh-scattered light from the sample surface, a 10-cm single monochromator with a resolution of 1.1 nm was used. The reflected light from the monochromator was detected by a Si photodetector with an electrical gain and the signal of the detector was amplified by a lockin amplifier. The combination of laser-power stabilizing systems and the lockin detection enables the discussion of the signals with the 10^{-6} order accuracy. All measurements were performed at room temperature (296 K).

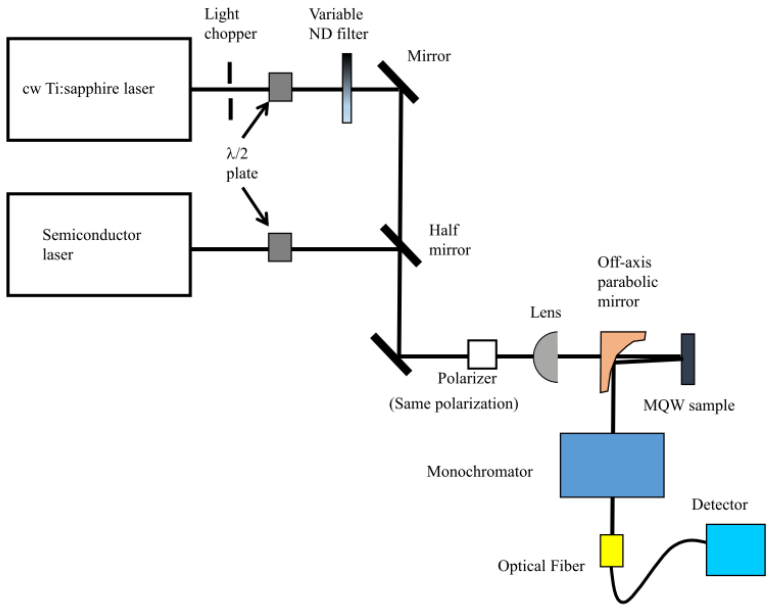

Figure 1. The experimental set-up to measure the reflectivity change signals. Two laser beams are combined on a half mirror.

3. Results and Discussion

Figure 2(a) shows the excitation-power dependence of the reflectivity change probed at the HH-exciton energy for various probe powers. The excitation laser was tuned to the LH-exciton energy. Both of the HH and LH excitons are created in the GaAs QWs. The reflectivity changes decreased as the probe power increased, with the maximum value observed for the 1-mW probe. The laser spectra are also provided in Fig. 2(b) for reference. As the excitation power increases, the reflectivity change increases for most probe powers. However, the reflectivity change also depends on the probe power, which is a key finding of this study.

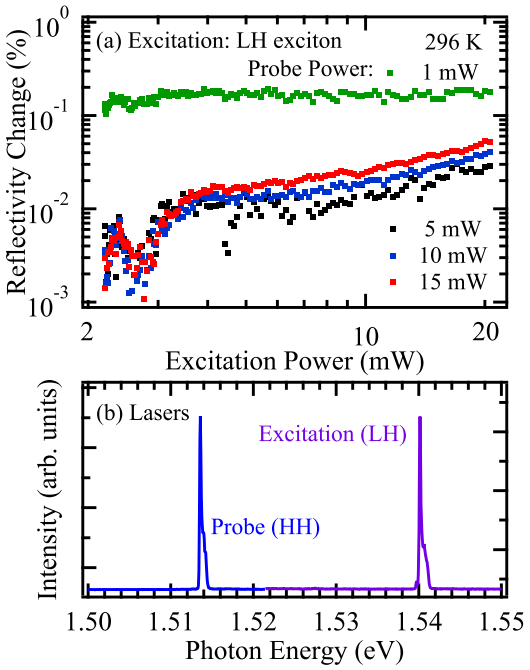

Figure 2. (a) Dependence of the reflectivity change on the LH-exciton excitation power, probed at the HH-exciton energy for various probe powers. (b) Laser spectra used in this measurement.

In general, the reflectivity is described as follows:

$$R = \frac{(n_1 - 1)^2 + n_2^2}{(n_1 + 1)^2 + n_2^2}, \tag{1}$$

where n_1 and n_2 are the refractive index and extinction coefficient, respectively. Using the real and imaginary parts of the complex dielectric function (ϵ_1 and ϵ_2), respectively, $n_1^2 = (\epsilon_1 + \sqrt{\epsilon_1^2 + \epsilon_2^2})/2$ and $n_2^2 = (-\epsilon_1 + \sqrt{\epsilon_1^2 + \epsilon_2^2})/2$ are described. The probe energy was fixed in the measurements; therefore, we can neglect the frequency-dependent term. Hence, the complex dielectric functions are written as $\epsilon_1 = 1 + \alpha N(I)$ and $\epsilon_2 = \beta N(I)$, respectively, where α and β are constants and $N(I)$ corresponds to the exciton density,

which depends on the excitation power. The trend of the exciton-density dependence of R at an exciton energy was obtained by these calculations, as shown by the thick solid curve in Fig. 2(a), which presents an example of the calculation. In this calculation, the multipole effect was not considered. Because the resonant probe is equal to the exciton energy, $\alpha = 0$ in this calculation. The calculation results indicate that the reflectivity varies with the exciton density corresponding to the excitation power, and this dependence does not remain constant.

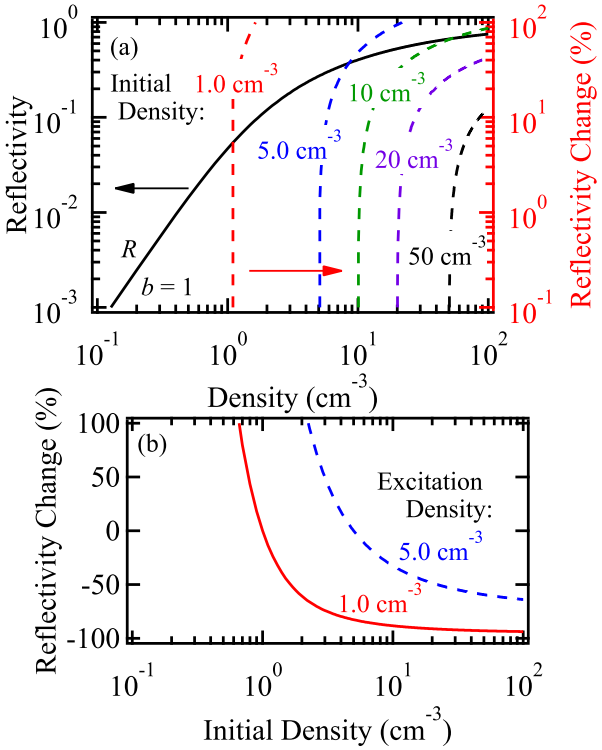

Figure 3. (a) Calculated reflectivity (solid curve) and reflectivity change (dashed and dotted curves) for $\alpha = 0$ and $\beta = 1$. (b) Reflectivity change as a function of initial exciton density for an excited exciton density of 1.0 (solid curve) and 5.0 (dashed curve) cm^{-3}.

To calculate the reflectivity change, ΔR, depending on the excitation density, the equation

$$\Delta R = \frac{R(N(I_{exc})) - R(N(I_{prb}))}{R(N(I_{prb}))} \tag{2}$$

was used. Here, $N(I_{exc})$ represents the exciton density at the probe energy created by the excitation-light illumination and $N(I_{prb})$ corresponds to the initial exciton density created by the probe light. The calculated results for various initial exciton densities are shown by the dashed curves in Fig. 2(a). While the value of the reflectivity change is different, the calculated dependence of the reflectivity change shows a similar shape

to the experimental results, with an approximately flat region appearing after the rapid increase. Therefore, considering the shape of profiles, the results of Fig. 2(a) originates from the increase in exciton number except for the weak excitation-power region in Fig. 2(a); where the reflectivity change demonstrates the dip structure. As the reason for this dip structure, it is speculated that the structure may come from the multipole effect neglected in the calculation.

Here, in the case of the dipole-type transition, such as excitons, β is related to the oscillator strength [38-41]. Hence, instead of the change in the exciton density due to the excitation light, it is possible to consider the variation of the oscillator strength due to the excitation light. However, even if the carriers by the excitation light change the exciton decay rate at the probe energy, which leads to the change in the oscillator strength, the variation is very small. Particularly, to show the rapid increase in the reflectivity change observed in the measurements, the oscillator strength should change largely, which is not easy. Furthermore, the positive reflectivity change is caused by the increase in the oscillator strength. From these reasons, the increase in the exciton density was considered as the major factor to cause the reflectivity change. In contrast, the change in the oscillator strength may be considered to obtain the correct value in the calculation.

The reflectivity change in Fig. 2(a) decreases with increasing probe power. In Fig. 3(a), the reflectivity change decreases as the density increases. Therefore, the decrease in the reflectivity change due to increasing probe power results from an increase in the initial occupation of the HH-exciton state. To confirm this finding, the dependence of the reflectivity change on the initial exciton density was calculated, as shown in Fig. 3(b), for excitation densities of 1.0 and 5.0 cm^{-3} by the solid and dashed curves, respectively. Although the reflectivity change values are very large, the reflectivity change primarily decreases with increasing initial density. In addition, the linear increase in the exciton by the excitation power was considered in the calculation. However, comparison with the experimental and calculation results may indicate that the increase of the probed exciton by the excitation light is more complex.

Here, we discuss the mechanism governing the increase in HH-exciton number. Two mechanisms are involved here: an intersubband transition and an in-plane transfer. To assess the difference in these effects, the signals were measured at various excitation energies for a probe power of 1 mW, as shown in Fig. 4(a). Here, the terms "2s exciton", which has smaller binding energy than the HH exciton which can be said "1s exciton" [42], and "p-layer" indicate excitation energies of 1.5266 and 1.5023 eV, respectively. The 2s exciton energy was evaluated using a low-temperature PL spectrum. The light with the energy of 1.5023 eV mainly excites the surface p-layer. Additionally, the term "HH exciton" denotes an excitation energy of 1.5163 eV, which is close to the probe energy of 1.5136 eV and excites the HH exciton within its inhomogeneous width. All laser spectra are shown in Fig. S1.

While the p-layer excitation shows different profiles for the low excitation-power region, with an almost linear increase, the profiles are similar at higher excitation powers.

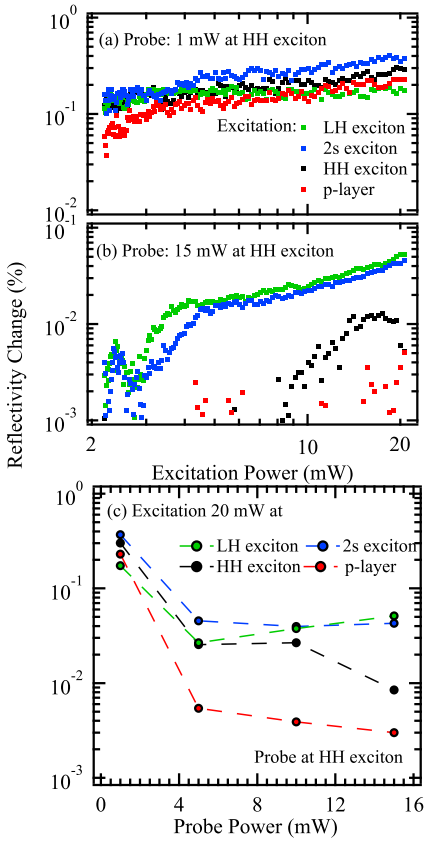

Figure 4. (a, b) Excitation-power dependence of the reflectivity change for various excitation energies. The probe power at the HH-exciton energy was 1 mW (a) or 15 mW (b). (c) Reflectivity change values for various excitation energies as a function of probe power at the HH exciton.

Based on the calculation results, this constant trend indicates that the number of HH excitons is sufficiently high. This result suggests that a large number of HH excitons are quickly supplied, even at lower excitation powers; therefore, the reflectivity increases little. If an HH exciton is created by the probe light, it is immediately ionized due to the internal electric field [37]. Therefore, the reflectivity change maintains an almost constant value.

As the probe power increases to 15 mW, the reflectivity modulation drastically changes, as shown in Fig. 4(b). Interestingly, the modulation by the excitation of the LH and 2s excitons shows a similar profile; the two-step increase appears due to the excitation of the LH and 2s excitons. On the other hand, while the HH-exciton and p-layer excitations do not show any excitation-power dependence at lower powers, the excitations show a rapid increase in the reflectivity change at higher excitation powers. As shown in Fig. S2, the signal becomes negative when the excitation power is smaller than the probe power, in agreement with calculations. Furthermore, the rapid increase is also in good agreement with calculations. Therefore, signals observed by intense probe

excitation correspond to an increase in exciton number.

For excitation of the LH and 2s excitons, an HH exciton caused by ionization is added to the original number of HH excitons created by the probe light tuned to the HH exciton energy. The ionization is caused by the thermal effects and internal field [37]. The intersubband transition from the LH to HH states occurs faster than in-plane diffusion. Therefore, the rapid increase in the reflectivity change is attributed to the intersubband transition. However, for the HH-exciton and p-layer excitations, an HH exciton due to in-plane transport is added. Because the supply rate corresponding to this movement is lower than that for the LH- and 2s-exciton excitations, a larger excitation power is needed to increase the reflectivity change.

The variation in the reflectivity change due to increasing probe power at the HH energy at an excitation power of 20 mW under various excitation energies is shown in Fig. 4(c). As the probe power is increased, the reflectivity change is decreased for all conditions, as shown in Fig. 3(b). Based on the DFM measurements [28], the THz signal is generated in the low-reflectivity-change region, i.e., the lower right region in Fig. 4(c). This case is different from that of two-mode laser oscillation, as mentioned above. Considering the preferable conditions for generating THz waves by the DFM mechanism, the overlap of two polarizations is essential. Therefore, the modulation should be small.

The free carriers may be considered as the origin of the modulation. At room temperature, excitons are rapidly ionized, and free electrons and holes are created [43, 44]. However, in the case of the quantum structures, such free carriers in QWs finally recombine as the excitons, which was observed as the square dependence of the PL intensity on the excitation power [44]. That was also observed in our sample, furthermore, exciton PL is dominant under the exciton-excitation conditions [37]. In addition, though the experiment was performed at low temperatures, it was shown that the resonant excitation could suppress the effect of free carriers [17]. Therefore, we are considering the free carriers hardly change the reflectivity at the exciton energies.

As another modulation mechanism, thermal excitation effects are also important. Indeed, the resonant excitation of the HH exciton causes the LH exciton PL [37]. Therefore, the reflectivity change signals probed at the LH-exciton energy were measured at the HH-exciton excitation energy, as shown in Fig. 5(a). The laser spectra are shown in Fig. 5(b). Unfortunately, we could not obtain a single-mode laser at this energy; thus, we used a multimode laser. However, the laser linewidth was much smaller than that of the LH exciton [37]. The monochromator used in the probe system is shown in Fig. 1. Hence, comparison with the results obtained at the HH exciton energy is possible. Considering the results of the resonant excitation PL [37], where the shift of the peak energies was not observed. Hence, it is possible to regard that the lattice temperature was almost constant during the laser input in the power region of our experiments.

The dependence in this case differs from that observed when probing at the HH-exciton energy. Particularly, while the reflectivity change is reduced for a probe power of 10 mW, the results for a probe power of 15 mW are larger than those for 5 and 10

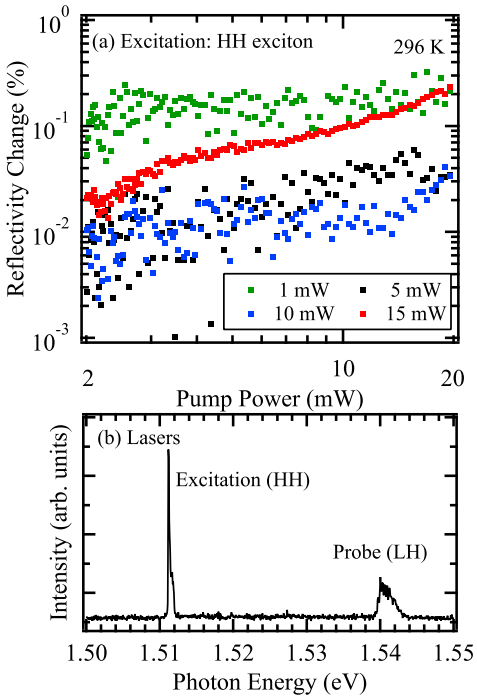

Figure 5. (a) Excitation-power dependence of the reflectivity change for various probe powers at the LH-exciton energy. (b) Laser spectra.

mW. Considering the calculation results, the initial decrease in the reflectivity change by 10 mW is attributed to an increase in the number of LH excitons, while the increase for the 15-mW probe results from a decrease in the number of LH excitons. This result indicates that the HH from the ionized HH exciton is thermally excited into the LH state.

To investigate the origin of the LH-exciton modulation, measurements were performed at various excitation energies, as shown in Figs. 6(a) and 6(b). For reference, the laser spectra are shown in Fig. S3. No rapid increase was observed for either probe power condition, in contrast to the HH-exciton probe measurements. This finding suggests that the number of LH excitons is maintained by suppressing the intersubband transition to the HH state because the HH state is occupied by the probe light, transiting from the 2s or p-layer excitons. On the other hand, the signals observed by the 1-mW probe under LH-exciton excitation and the 15-mW probe show an almost linear dependence on the excitation power. These results indicate that the intense probe light causes the annihilation of the LH exciton due to exciton-exciton scattering.

Figure 6(c) presents a summary of the results obtained by the LH probe. Except for the case of LH excitation, the reflectivity change increases for a probe power of 15 mW, which is different from the dependence shown in Fig. 3(b). This increase in probe power does not cause an increase in the reflectivity change. Therefore, the intense probe power causes exciton annihilation at the LH-exciton energy. In contrast, the reflectivity

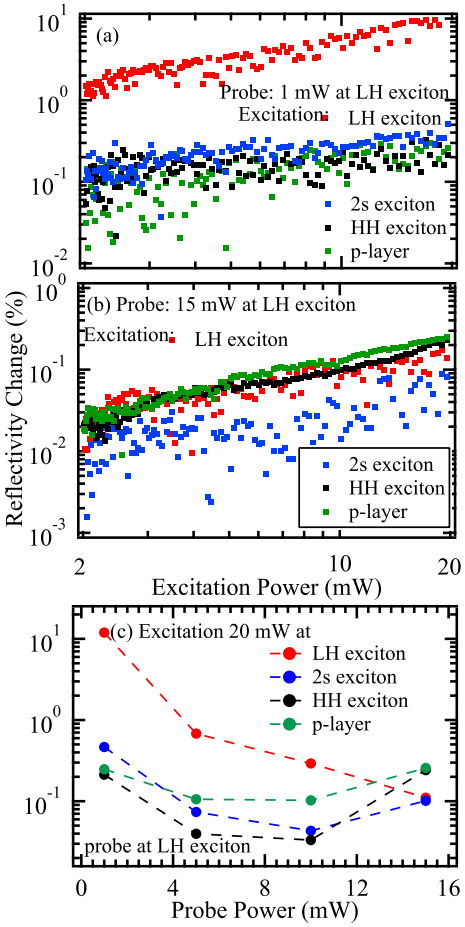

Figure 6. (a, b) Excitation-power dependence of the reflectivity change for various excitation energies. The probe power at the LH-exciton energy was 1 mW (a) or 15 mW (b). (c) Reflectivity change for various excitation energies as a function of probe power at the LH exciton.

change increases with increasing excitation power for all excitation energies. This result demonstrates that the LH exciton is supplied by the thermal excitation of carriers due to ionized excitons or carriers in the p-layer. In DFM measurements, this supply is important for generating THz signals to ensure that the nonlinear polarization is stable.

4. Conclusion

We have investigated the interaction between excitons excited by cw lasers by measuring the reflectivity change in a GaAs/AlAs MQW at room temperature. The increase in reflectivity change due to increasing excitation power originates from an increased number of excitons in agreement with calculations. Interestingly, the profiles of excitation-power dependence varied with probe power. Moreover, the dependence

probed at the HH-exciton energy differs from that probed at the LH-exciton energy, due to a difference in the modulation mechanism. Our results demonstrate that the initial exciton density, which depends on the probe power, is an important factor to consider when setting spectroscopic measurement conditions. Furthermore, these results have clarified why intense cw laser beams are required to generate an intense DFM-THz signal, thus, elucidating why the resonant effect at the HH- and LH-exciton excitation condition is weak. Therefore, to enhance THz signals by DFM, the exciton number must be carefully controlled.

Calculation can roughly explain the trend. However, to explain the more detailed change the multipole effects should be included.

Acknowledgments

We would like to acknowledge financial support provided by JSPS KAKENHI Grant Numbers 26289088, 16KK0129 and 19K04532, the JSPS International Research Fellow (Graduate School of Engineering, Kobe University), Masuya-Kinen Basic Research Foundation, Sasakura Enviro-Science Foundation, Kawanishi Memorial ShinMaywa Education Foundation and Support Center for Advanced Telecommunications Technology Research Foundation. The author would like to thank Enago for the English language review.

References

[1] Leo K., Damen T. C. and Shah J. 1990 Quantum beats of light hole and heavy hole excitons in quantum wells *Appl. Phys. Lett.* **57**, 19

[2] Brener I., Planken P. C. M., Nuss M. C., Pfeiffer L., Leaird D. E. and Weiner A. M. 1993 Repetitive excitation of charge oscillations in semiconductor heterostructures *Appl. Phys. Lett.* **63** 2213

[3] Paul A. E., Sha W., Patkar S. and Smirl A. L. 1995 Excitation-induced phase shifts of heavy- and light-hole quantum beats in GaAs/AlxGa1-xAs multiple quantum wells *Phys. Rev. B* **51** 4242

[4] Kim D. S., Sohn J. Y., Yahng J. S., Ahn Y. H., Yee K. J., Yee D. S., Jho Y. D., Hohng S. C., Kim D. H., Kim W. S., Woo J. C., Meier T., Koch S. W., Woo D. H., Kim E. K., Kim S. H. and Kim C. S. 1998 Femtosecond Four-Wave Mixing Experiments on GaAs Quantum Wells Using Two Independently Tunable Lasers *Phys. Rev. Lett.* **80**, 4803

[5] Kojima O., Mizoguchi K. and Nakayama M. 2003 Coupling of coherent longitudinal optical phonons to excitonic quantum beats in GaAs/AlAs multiple quantum wells *Phys. Rev. B* **68**, 155325 (2003).

[6] Kojima O., Mizoguchi K. and Nakayama M. 2004 Dephasing mechanisms of Bloch oscillations in GaAs/$Al_{0.3}Ga_{0.7}$As superlattices investigated by time-resolved terahertz spectroscopy *Phys. Rev. B* **70**, 233306

[7] Hasegawa T., Mizoguchi K. and Nakayama M. 2007 Transformation process from quantum beats of miniband excitons to Bloch oscillations in a GaAs/AlAs superlattice under applied electric fields *Phys. Rev. B.* **76** 115323

[8] Spivey A. G. V. and Cundiff S. T. 2007 Inhomogeneous dephasing of heavy-hole and light-hole exciton coherences in GaAs quantum wells *J. Opt. Soc. Am. B* **24** 664

[9] Kojima O., Isu T., Ishi-Hayase J., Kanno A., Katouf R., Sasaki M., Tsuchiya M. 2008 Ultrafast response induced by interference effects between weakly confined exciton states *J. Phys. Soc. Jpn.* **77** 044701

[10] Priyadarshi S., Pierz K., Siegner U., Dawson P. and Bieler M. 2011 All-optical generation of coherent in-plane charge oscillations in GaAs quantum wells *Phys. Rev. B* **83** 121307 (2011).
[11] Turner D. B., Wen P., Arias D. H., Nelson K. A., Li H., Moody G., Siemens M. E. and Cundiff S. T. 2012 Persistent exciton-type many-body interactions in GaAs quantum wells measured using two-dimensional optical spectroscopy *Phys. Rev. B* **85** 201303
[12] Ohta S., Kojima O., Kita T. and Isu T. 2012 Observation of quantum beat oscillations and ultrafast relaxation of excitons confined in GaAs thin films by controlling probe laser pulses *J. Appl. Phys.* **111** 023505
[13] Kojima O., Mizoguchi K. and Nakayama M. 2012 Quantum beats of type-I and type-II excitons in an $In_xGa_{1-x}As$/GaAs strained single quantum well *J. Appl. Phys.* **112** 043522.
[14] Khan S., Jayabalan J., Chari R., Pal S., Porwal S., Sharma T. K. and Oak S. M. 2014 Quantum beats from the coherent interaction of hole states with surface state in near-surface quantum well *Appl. Phys. Lett.* **105** 073106
[15] Kojima O., Kojima K., Kita T. and Akahane K. 2015 Rapid dephasing related to intersubband transitions induced by exciton quantum beats observed by a pump-probe technique in a GaAs/AlAs multiple quantum well *Phys. Rev. B* **91** 125307
[16] Kojima O. and Kita T. 2016 Effects of exciton line widths on the amplitude of quantum beat oscillations *Appl. Phys. Express* **9** 062801
[17] Kojima O., Iwasaki Y., Kita T. and Akahane K. 2017 Effects of non-exciton components excited by broadband pulses on quantum beats in a GaAs/AlAs multiple quantum well *Sci. Reps.* **7** 41496
[18] Sim S., Lee D., Trifonov A. V., Kim T., Cha S., Sung J. H., Cho S., Shim W., Jo M.-H. and Choi H. 2018 Ultrafast quantum beats of anisotropic excitons in atomically thin ReS2 *Nature Commun.* **9** 351
[19] Feldmann J., Leo K., Shah J., Miller D. A. B., Cunningham J. E., Meier T., von Plessen G., Schulze A., Thomas P. and Schmitt-Rink S. 1996 Optical investigation of Bloch oscillations in a semiconductor superlattice *Phys. Rev. B* **46** 7252
[20] Leisching P., Bolivar P. H., Beck W., Dhaibi Y., Brüggemann F., Schwedler R., Kurz H., Leo K. and Köhler K. 1994 Bloch oscillations of excitonic wave packets in semiconductor superlattices *Phys. Rev. B.* **50** 14389
[21] Cohen G., Bar-Joseph I. and Shtrikman H. 1994 Stark ladder and temporal oscillations in a narrow-band superlattice *Phys. Rev. B.* **50** 17316
[22] Fanciulli R., Weiner, Dignam M. M., Meinhold D. and Leo K. 2005 Coherent control of Bloch oscillations by means of optical pulse shaping *Phys. Rev. B* **71** 153304
[23] Gu P., Tani M., Hyodo M., Sakai K. and Hidaka T. 1998 Generation of cw-Terahertz Radiation Using a Two-Longitudinal-Mode Laser Diode *Jpn. J. Appl. Phys.* **37** L976
[24] Hoffmann S. and Hofmann M. R. 2007 Generation of Terahertz radiation with two color semiconductor lasers *Laser Photon. Rev.* **1** 44
[25] Kruczek T., Leyman R., Carnegie D., Bazieva N., Erbert G., Schulz S., Reardon C., Reynolds S. and Rafailov E. U. 2012 Continuous wave terahertz radiation from an InAs/GaAs quantum-dot photomixer device *Appl. Phys. Lett.* **101** 081114
[26] Kitada T., Katoh S., Takimoto T., Nakagawa Y., Morita K. and Isu T. 2013 Terahertz emission from a GaAs/AlAs coupled multilayer cavity with nonlinear optical susceptibility inversion *Appl. Phys. Lett.* **102** 251118
[27] Liu B., Bromberger H., Cartella A., Gebert T., Först M. and Cavalleri A. 2017 Generation of narrowband, high-intensity, carrier-envelope phase-stable pulses tunable between 4 and 18 THz *Opt. Lett.* **42** 129
[28] Kojima O., Tarui Y., Shimazu H., Kita T., Majeed A., Ivanov P., Clarke E., Hogg R. 2018 Wide frequency tuning of continuous terahertz wave generated by difference frequency mixing under exciton-excitation conditions in a GaAs/AlAs multiple quantum well *Phys. Rev. Appl.* **10** 044035
[29] Majeed A., Ivanov P., Stevens B., Clarke E., Butler I., Childs D., Kojima O., Hogg R. 2019

Broadband THz absorption spectrometer based on excitonic nonlinear optical effects *Light: Sci. Appl.* **8** 29

[30] Alouini M., Bretenaker F., Brunel M., Le Floch A., Vallet M. and Thony P. 2000 Existence of two coupling constants in microchip lasers *Opt. Lett.* **25**, 896 (2000).

[31] Brunel M., Amon A. and Vallet M. 2005 Dual-polarization microchip laser at 1.53 μm *Opt. Lett.* **30** 2418

[32] Pal V., Trofimoff P., Miranda B.-X., Baili G., Alouini M., Morvan L., Dolfi D., Goldfarb F., Sagnes I., Ghosh R. and Bretenaker F. 2010 Measurement of the coupling constant in a two-frequency VECSEL *Opt. Express* **18** 5008

[33] Chusseau L. and Philippe F. 2013 Mode competition in a dual-mode quantum-dot semiconductor microlaser *Phys. Rev. A* **88**, 015803

[34] De S., Potapchuk V. and Bretenaker F. 2014 Influence of spin-dependent carrier dynamics on the properties of a dual-frequency vertical-external-cavity surface-emitting laser *Phys. Rev. A.* **90** 013841

[35] Chusseau L., Vallet A., Perrin M., Paranthoën C. and Alouini M. 2018 Lamb mode-coupling constant in quantum-dot semiconductor lasers *Phys. Rev. B* **98** 155306

[36] Brëvalle G., Pes S., Paranthoën C., Perrin M., Levallois C., Hamel C., Mereuta A., Caliman A., Kapon E., Vallet A. Chusseau L. , Folliot H. and Alouni M. 2019 Direct measurement of the spectral dependence of Lamb coupling constant in a dual frequency quantum well-based VECSEL *Opt. Express* **27**121083

[37] Kojima O., Kita T., Steer M. J. and Hogg R. A. 2020 Resonant exciton excitation photoluminescence and dynamics in a GaAs/AlAs multiple quantum well with internal electric field *AIP Advances* **10** 095016

[38] Ivchenko E. L., Kochereshko V. P., Kop'ev P. S., Kosobukin V. A., Uraltsev I. N. and Yakovlev D. R. 1989 Exciton longitudinal-transverse splitting in GaAs/AIGaAs superlattices and multiple quantum wells *Solid State Commun.* **70** 529

[39] Gil B., Khalifi Y. El, Mathieu H., de Paris C., Massies J., Neu G., Fukunaga T. and Nakashima H. 1990 Line-shape analysis of the refiectivity spectra of GaAs/(Ga, A1)As single quantum wells grown on (001)- and (311)-oriented substrates *Phys. Rev. B* **41** 2885

[40] Andreani L. C. 1991 Radiative lifetime of free excitons in quantum wells *Solid State Commun.* **77** 641

[41] Schaefer A. C. and Steel D. G. 1997 Nonlinear optical response of the GaAs exciton polariton *Phys. Rev. Lett.* **79** 4870

[42] Dawson P., Moore K. J., Duggan G., Ralph H. I., and Foxon C. T. B. 1986 Unambiguous observation of the 2s state of the light- and heavy-hole excitons in GaAs-(AlGa) As multiple-quantum-well structures *Phys. Rev. B* **34**, 6007

[43] Chemla D. S. and Miller D. A. B. 1985 Room-temperature excitonic nonlinear-optical effects in semiconductor quantum-well structures *J. Opt. Soc. Am B* **2** 1155

[44] Fouquet J. E. and Siegman A. E. 1985 Room- temperature photoluminescence times in a GaAs/$Al_xGa_{1-x}As$ molecular beam epitaxy multiple quantum well structure *Appl. Phys. Lett.* **46** 280